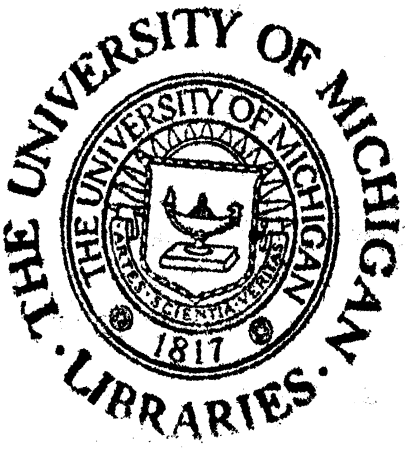

ARPA Order No. 1244

Program Code No. 8D10

Name of Contractor: The Regents of The University of Michigan

Effective Date of Contract: July 1, 1968

Contract Expiration Date: May 31, 1970

Amount of Contract: $83,333.00

Contract No. F33615-68-C-1703

Principal Investigator: J. R. Frederick
Phone: 313-764-3387

Short Title of Work: Use of Acoustic Emission in Nondestructive Testing

## FOREWORD

This is the first semiannual report on a study of the use of acoustic emission in nondestructive testing. This research is supported by the Advanced Research Project Agency of the Department of Defense and is monitored by the Air Force Materials Laboratory, MANN, under Contract No. F33615-68-C-1703, initiated under ARPA Order 1244, Program Code 8D10. Mr. R. R. Rowand (MANN) is project engineer. This report covers the period from July 1, 1968 to February 28, 1969.

The program is being carried out in the Rheology and Fracture Laboratories of the Mechanical Engineering Department at The University of Michigan. The work is under the direction of Associate Professor J. R. Frederick. Professor David K. Felbeck, Dr. A. Agarwall, Mr. G. Sankar, and Mr. M. Shah have participated in the program.

ABSTRACT

The objective of the program is to investigate the feasibility of the use of acoustic emission as a nondestructive testing tool. A model is proposed in order to explain the acoustic emission which results from dislocation motion. The model is used to predict the minimum dislocation source length and the minimum slip region radius that is capable of producing detectable acoustic emission. Agreement is obtained between the model and experimental results on 99.99% aluminum and 2024 aluminum alloy. Data have been obtained on the acoustic emission from various alloys during the removal of the stress from a test specimen. This effect appears to be related to the magnitude of the Bauschinger effect in these materials.

TABLE OF CONTENTS

LIST OF FIGURES

## I. INTRODUCTION

Acoustic emission from materials is produced as a result of (1) crack nucleation or propagation, (2) dislocation motion, (3) phase transformations, and (4) twinning. The acoustic emission work that is being pursued at The University of Michigan is concerned primarily with the emission caused by dislocation motion. The principal effort is directed toward obtaining a better understanding of the mechanisms that are involved in acoustic emission from this type of source and correlating the microstructure and the mechanical behavior of materials with the characteristics of the acoustic emission.

## II. PRESENT TASKS

### A. DEVELOPMENT OF A MODEL FOR ACOUSTIC EMISSION BASED ON DISLOCATION MOTION

A simple model for acoustic emission that has been proposed by Agarwal[1] is being extended to predict the minimum dislocation source length and the minimum slip region radius that can result in detectable acoustic emission.

#### The Model

Well annealed materials contain about $10^6$ dislocations per square centimeter which are usually distributed in a three-dimensional network, the Frank network. Prolonged thermal treatment at an elevated temperature allows dislocations to be annihilated or to move into this low energy configuration. Mott[2] showed that it is geometrically possible for three dislocations to meet in a point and form a node. A random array of dislocations can thus change during annealing to a rather stable three-dimensional network. The dislocations that make up the network can be further pinned by impurity atoms or precipitate particles, so as to

substantially reduce the average free dislocation length. It is assumed that the pinning resulting from the nodes of the network and hard precipitates is so strong that no break-away of dislocation segments occurs under the action of an applied stress. Dislocations may, however, break away from the impurity atoms.

Observations of thin foils by electron microscopy show that in most cold-worked metals a three-dimensional network of dislocations is developed. This is analogous to the Frank network but on a much smaller scale, and the dislocations may be more non-uniformly distributed after cold-work. This smaller network is also stable at temperatures below about half the melting temperature, but at higher temperatures dislocations can climb and glide more easily. Thus, at high temperatures most of the dislocations can be annihilated, and the total length of dislocations will be much smaller. The final average length of dislocation segments is thus much larger in annealed material than in the cold-worked material.

The exact form of the slip that causes the elastic pulses cannot be determined from these tests, but it is possible to estimate the minimum detectable elastic strain, and from this the magnitude of local slip that caused it.

The piezoelectric stress constant, $g_{33}$ is defined by

$$g_{33} = \frac{\bar{v}}{\sigma} \tag{1}$$

$\bar{v}$ = volts per meter length of crystal

$\sigma$ = stress, newtons per square meter

Let the threshold or minimum detectable output voltage of the crystal above the noise level be $v_{min}$, $\epsilon_x$ the strain in the crystal, and $E_x$ the elastic modulus of the crystal. The minimum detectable average displacement $\delta_{min}$ of the crystal of length h is

$$\delta_{min} = \epsilon_x h$$

$$= \left| \frac{\sigma}{E_x} \right| h$$

Substituting for $\sigma$ from Eq. (1) we get $\delta_{min} = \frac{\bar{v}}{g_{33} E_x} h$

$$\bar{v} = \frac{v_{min}}{h}$$

$$\delta_{min} = \frac{v_{min}}{g_{33} E_x} \tag{2}$$

For the equipment used in this study

$$v_{min} = 4 \text{ microvolts}$$

$$g_{33} = 24.4 \times 10^{-3} \ \frac{\text{volt-meter}}{\text{newton}}$$

$$E_x = 5.85 \times 10^{10} \ \text{newton/meter}^2$$

hence, the minimum detectable displacement is

$$\delta_{min} = \frac{4 \text{ microvolts}}{24.4 \times 10^{-3} \times 5.85 \times 10^{10}}$$

$$= 2.8 \times 10^{-15} \text{ meter}$$

In an aluminum specimen of 3-in. deformed length, the average strain $\epsilon$ corresponding to this detectable displacement is

$$\epsilon = \delta_{min}/\text{length} = \frac{2.8 \times 10^{-15} \text{m}}{3 \times 0.0254 \text{ m}} = 3.67 \times 10^{-14}$$

If the probable losses in the system are considered, the minimum detectable levels of strain are probably one or two orders of magnitude larger.

It is possible to make an estimate of the minimum size of active slip system that can be detected by this equipment. For simplicity, assume a Frank-Read source that operates until a pileup occurs that shuts it off.

Let the initial length of the source be f, so that f/2 will be the minimum radius of curvature of the dislocation when the source becomes unstable. The local shear stress $\tau$ for this condition is of the order of

$$\tau = \frac{Gb}{f/2} \tag{3}$$

where G is the shear modulus of elasticity and b the Burgers vector of the dislocation. Let the maximum glide distance of the first dislocation be L. Then the outside diameter of the slip region will be 2L. If the local stress $\tau$ that causes the source to become unstable is assumed to be the same as the average stress acting over the slip region after the source is stopped, then the number n of dislocations in the final pileup of length L can be estimated. The number of dislocations in a pileup that stops the source is given by

$$n = \frac{\pi \tau L}{Gb}$$

Combining this with the stress Eq. (3) we get

$$n = \frac{2\pi L}{f} \tag{4}$$

Consider a $\{111\}$ slip plane with its normal at 45 degrees to the applied axial tensile stress in a cylindrical specimen. For $\{111\}\langle 110\rangle$ slip in aluminum, the condition of minimum axial tensile stress for slip is achieved when a $\langle 110\rangle$ direction is at 45 degrees to the axial applied stress. When a source of this orientation produces n dislocations, each moving an average distance of (3/4) L, the average axial displacement $\delta$ at a distance of several specimen diameters away from the slip region is shown in Fig. 1 . It can be seen that the average strain due to slip over the slip plane is

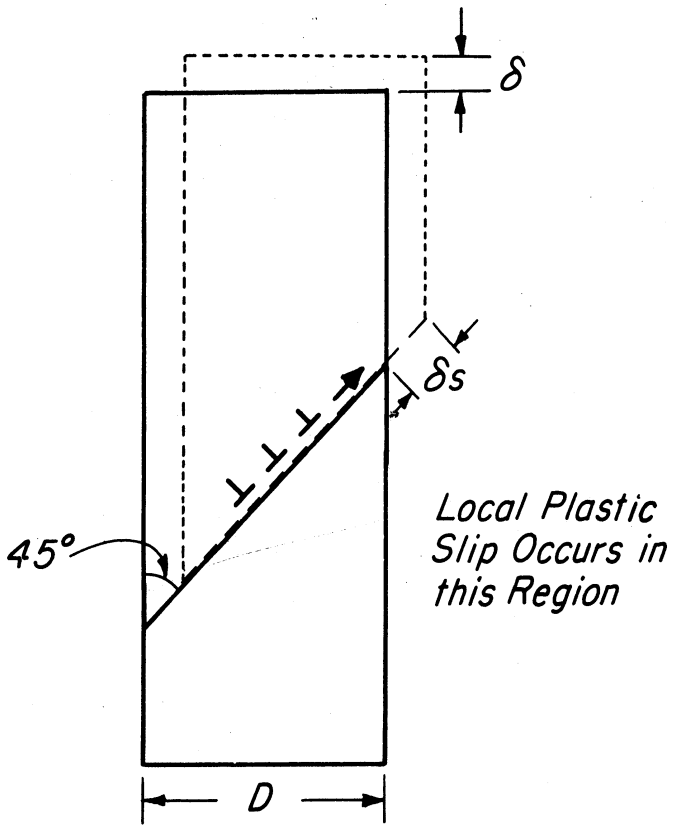


Fig. 1. The slip of n dislocations on a plane at 45° to the tensile axis will produce an axial displacement δ at a distance of several specimen diameters away from the slip region.

$$\delta_s = \frac{nb\ A_s}{A/\cos 45^\circ} \tag{5}$$

where A is the cross sectional area of the specimen, and the average area, $A_s$, swept out by each dislocation is

$$A_s = \pi(3L/4)^2 .$$

The calculation of $A_s$ neglects the error resulting from squaring the average glide distance for the pileup rather than using the weighted average area over which slip occurs.

Substituting $A_s$ in Eq. (5) gives

$$\delta_s = \frac{9\pi nbL^2}{16\sqrt{2A}}$$

The average axial displacement $\delta$ for this case is then

$$\delta = \delta_s/\sqrt{2}$$

$$= \frac{9\pi}{32}\frac{nbL^2}{A}$$

Combining this with Eq. (4) gives

$$\delta = \frac{9\pi^2}{16}\frac{bL^3}{fA}$$

If this displacement is set equal to the minimum detectable displacement of the PZT5 piezoelectric crystal given by Eq. (2) a general expression for L and f results:

$$L^3 = \frac{16}{9\pi^2}\left(\frac{v_{min}}{g_{33}E_x}\right)\frac{A}{b}f \tag{6}$$

L is the maximum glide distance (half the slip region diameter), in meters, $v_{min}$ is the threshold crystal output voltage, 4 microvolts in these tests, the piezoelectric stress constant $g_{33} = 24.4 \times 10^{-3}$ v-m/n, the crystal modulus $E_x = 5.85 \times 10^{10}$ n/m$^2$, the cross sectional area of the specimen

$A = 31.7 \times 10^{-6}$ $m^2$, the Burgers vector $b = 2.86 \times 10^{-10}$ m, and f is the free length of the dislocation source in meters.

With the constants that apply for these tests, Eq. (6) reduces numerically to:

$$L^3 = (55.3 \times 10^{-12})f \tag{7}$$

This relationship appears as a solid straight line on the log-log plot in Fig. 2. It represents the minimum slip region radius, L, that will give detectable emission for a single given source length f. A single source has been considered here because the probability of a time overlap during the operation of sources in the plastic microstrain region is very small. Each source stops within about 10-15 microsec once it becomes operative.

Consider now the limitations on the ratio L/f. Dislocations in annealed polycrystalline metals will be found as networks, pinned either by the network or by local defects or particles. Thus, the free length of dislocation will be limited. In the same way the maximum possible glide distance for an expanding source will also be limited. If fine particles limit the glide distance L, then L/f may be of the order 10. If the Frank network limits L, then L/f will probably be closer to unity. A line is drawn on Fig. 2 representing L/f = 10 as a reasonable maximum value for L, for a given dislocation source length f. It should be noted that these strains are far below the general yield region, where large slip lengths are observed.

Thus, the solid threshold line in Fig. 2 provides a lower bound for detectable emission and the line L = 10f provides an upper bound for plausible slip systems in the microstrain region. The area bounded by these lines, shown shaded by coarse cross hatching in Fig. 2, thus provides the

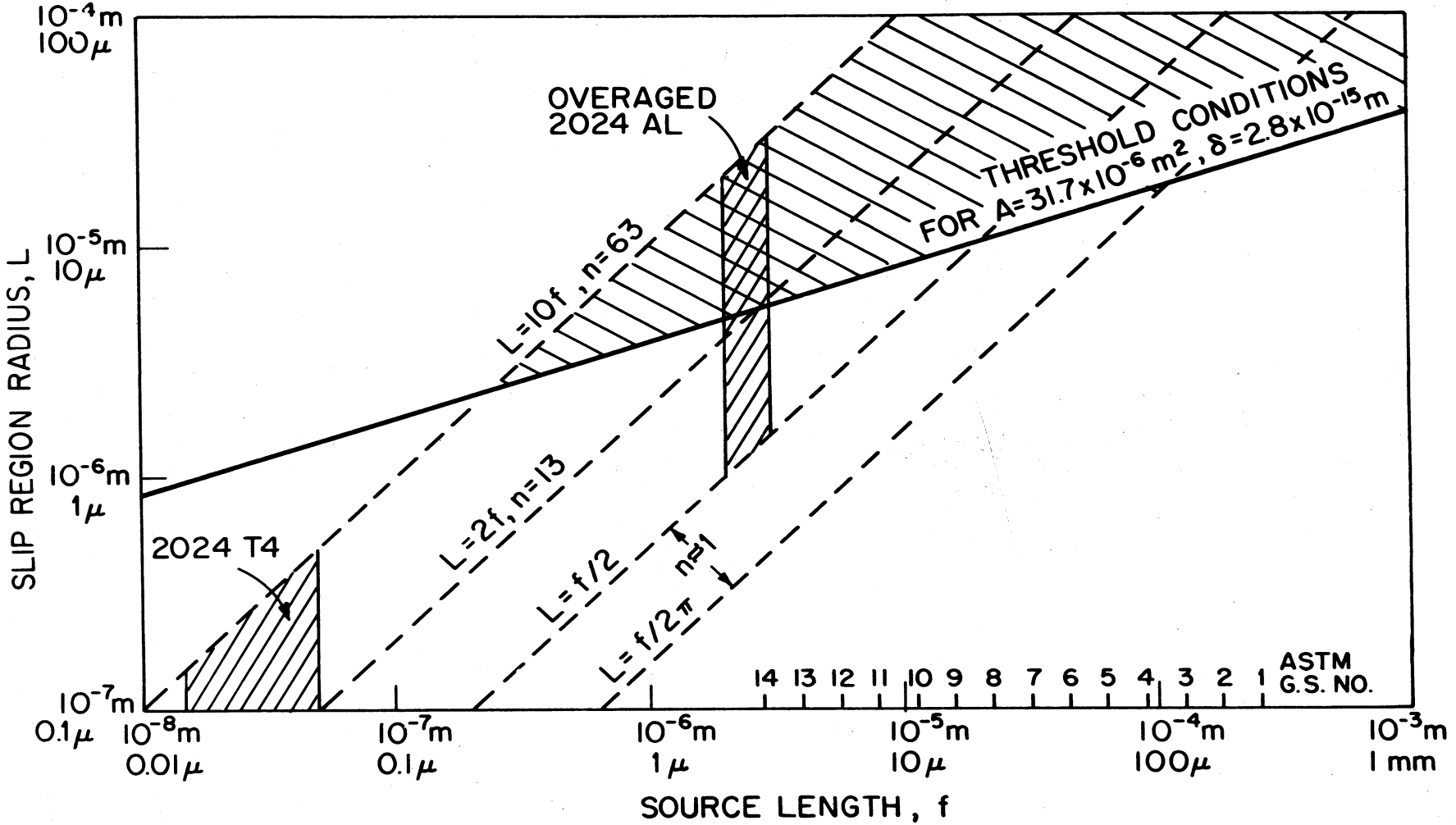


Fig. 2. The minimum slip region radius, L, that will give detectable emission depends on the length of the source, f. The solid line in the figure represents the threshold for detectable emission. No emission would be observed for points lying below this line. The region in which possible slip can be detected is shown by the coarse shading.

region where possible slip can be detected. For the values used in this analysis, the graph suggests that no acoustic emission can be detected from sources of length less than about $2.5 \times 10^{-7}$ m, or 0.25 micron.

Application of The Model to Test Results

Annealed superpurity (99.99%) aluminum: High values of acoustic emission have been measured for this material which indicates the presence of sources greater than 0.25 microns in length, in fact probably of the order of 10-100 microns. This falls in the range of grain sizes normally encountered, and the region of detectable emission shown in Fig. 2 shows that a wide range of L/f can be expected to give measurable emission. Both air-cooled and furnace-cooled specimens of this material give detectable emission and this suggests that even if the impurities have some pinning effect, the source lengths that are encountered are still large enough to be detected. (A parallel series of tests on 2024 aluminum, not reported here, shows that water quenching from 975°F (524°C) results in large load emission but air- and furnace-cooling from the same temperature apparently allow enough precipitation of impurities to prevent detectable load emission from occurring.)

Cold-worked superputity aluminum: If it is assumed, for purposes of very rough calculation, that the increase in dislocation density as a result of cold-work produces a uniform simple cubic network of progressively smaller unit size, it is possible to make an estimate of the highest dislocation density for which acoustic emission can be detected in these tests. A reasonable value of L/f for such a network may be taken as 2 (see argument above). Fig. 2 gives the three minimum detectable source length as about microns. For a cubic cell side dimension d in this assumed network, a $\{100\}$ intersection will give a dislocation density of $\rho_1 = 1/d^2$. For a $\{110\}$ intersection, the density will be

$$\rho_2 = \frac{2}{d^2}\Big/\sqrt{2} = \sqrt{2}/d^2 .$$

And for a $\{111\}$ intersection, the density will be

$$\rho_3 = \frac{3}{2d^2}\Big/\sqrt{3/2} = \frac{\sqrt{3}}{d^2} .$$

Use as a rough mean $\rho = 1.5/d^2$. If d = 3 microns,

$$\rho = 1.5/(3 \times 10^{-4} \text{ cm})^2 = 1.7 \times 10^7/\text{cm}^2$$

This value is not much larger than the dislocation density in the annealed material and suggests that very little cold work will eliminate detectable load emission. This has been observed in all tests conducted to date, even when the test loading is not in the same orientation as the cold-work deformation loading.

Naturally aged 2024 aluminum: As the precipitates form with time following solution heat treating, the maximum value of f decreases until it is less than 0.25 micron. Alloys of this composition are known to have an average particle spacing[3] in the range 0.015 - 0.050 microns. If f is of the same order of magnitude as the particle spacing, then Fig. 2 indicates that no emission should be detectable from a fully aged 2024 aluminum alloy. The fine cross-hatched region for 2024-T4 does in fact fall well below the threshold curve. Partially aged 2024 should give a limited amount of detectable emission because the particles would be expected to have average spacing in the micron range. This agrees with the experimental results obtained by Agarwal[1] as shown in Fig. 3.

Overaged 2024 aluminum: Aging Al-4% Cu at 572°F (300°C) for one hour or Al-4.6% Cu at 482°F (250°C) for 48 hours gives an average $CuAl_2$ particle spacing in the range 1.0 - 2.5 microns. The aging treatment in these experiments at 600°F (316°C) for 100 hr may therefore result in slightly higher spacing, namely in the range of 2-3 microns. Fig. 2 shows that

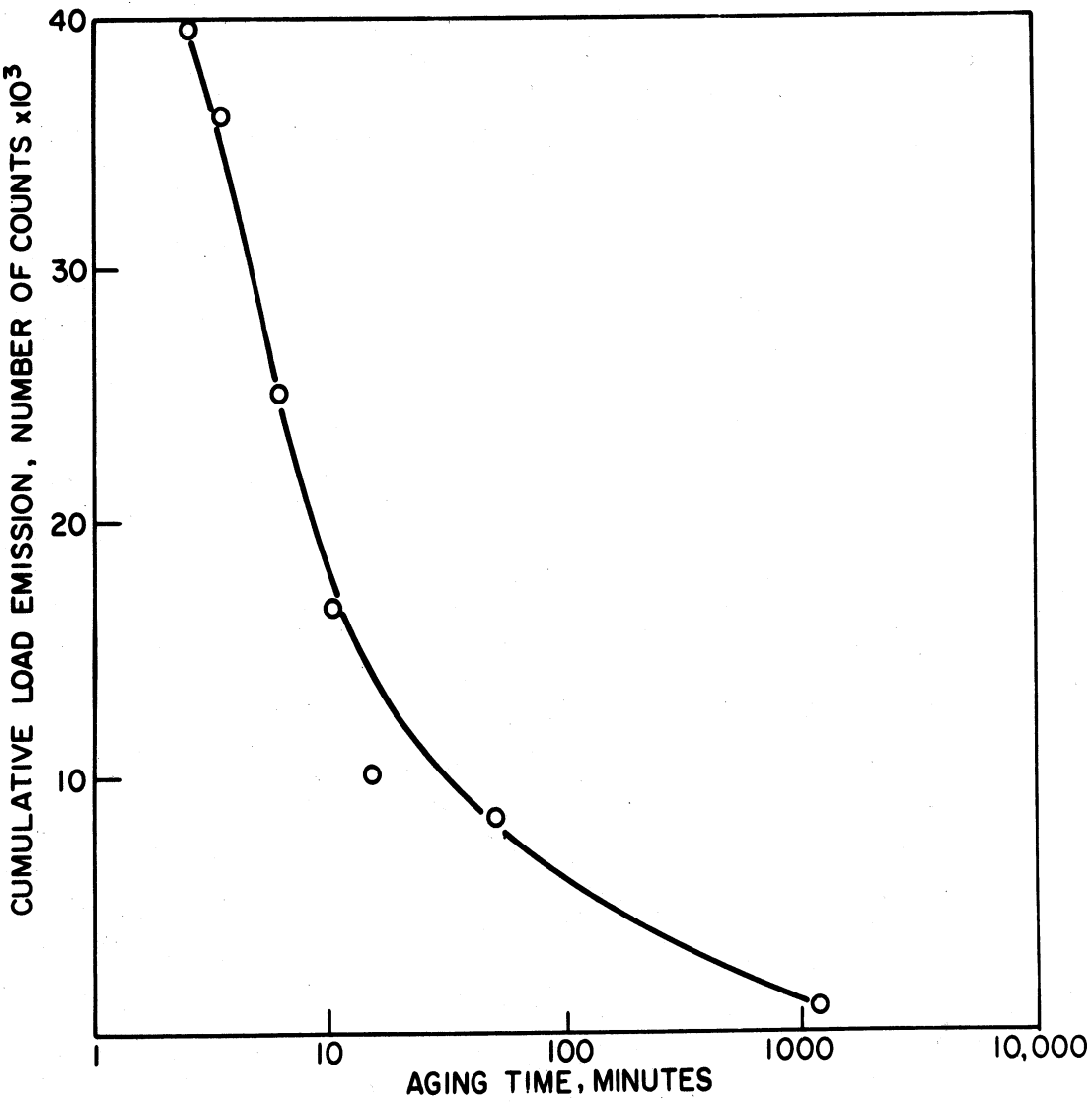


Fig. 3. Dependence of the cumulative load emission from 2024 aluminum on aging time.

part of this region falls within the detectable range and part below the threshold. The tests give a small but unquestionable number of acoustic emissions for this condition.

Effect of Grain Size: It is expected that a correlation between grain size or sub-grain size and the acoustic emission will also be obtained because of the effect of grain boundaries on limiting the amount of possible slip. The techniques for producing aluminum specimens having controlled grain sizes are being developed and the data obtained so far indicate that the effect of grain size on emission may be explained by the model.

## B. CORRELATION OF THE ACOUSTIC EMISSION OBTAINED ON UNLOADING A SPECIMEN WITH THE MAGNITUDE OF THE BAUSCHINGER EFFECT

Acoustic emission is observed not only when stress is applied to a test specimen but it has also been observed when the stress is removed. Furthermore, this unload emission occurs at levels of stress that are below the gross yield stress. The dependence of the magnitude of this emission on the amount of plastic strain is shown in Fig. 4 for various metals. Each point on the graph indicates the emission that is observed when the load which produced the indicated amount of strain is removed. An explanation of this emission appears to be possible on the basis of the Bauschinger effect.

One measure of the Bauschinger effect is the reduction in the compressive yield stress of a test specimen which is first tested in tension and then in compression. Another manifestation of the effect occurs in those materials that show a "reverse plastic flow" when the load is removed during a tensile or compression test. It has also been observed that those materials which show a Bauschinger effect also exhibit "planar" slip while other materials exhibit "wavy" slip.

The materials showing a high unload acoustic emission in Fig. 4, namely, magnesium, Cu - 7.9 Al alloy, and 70-30 brass were purposely chosen because they exhibit planar slip and are known to show a significant Bauschinger effect during conventional stress-strain tests. The 6061 alloy and the superpurity aluminum showed less unload emission and are known to exhibit wavy slip. Suitable data in the Bauschinger effect in these two materials could not be found.

Experiments are in progress to determine the magnitude of the Bauschinger effect for the materials shown in Fig. 4 at the plastic strain levels shown on the graph. A direct comparison will then be made between the unload emission and the magnitude of the Bauschinger effect.

### C. ACOUSTIC EMISSION DURING CYCLIC FATIGUE

Work on the observation of acoustic emission during cyclic fatigue is in progress. An electrodynamic vibration generator is being used. The test specimens are flat and are mounted as a cantilever beam. Initial tests are being performed on 1100-H14 aluminum specimens. The acoustic emission is monitored continuously by means of a CLEVITE PZT-5 transducer mounted at the base of the specimen. Preliminary results indicate that the emission tends to be large at the beginning and at the end of a fatigue test and low in the middle of the test.

## III. FUTURE WORK

The programs that have been described are being continued. New tasks to be undertaken are: (1) an investigation of acoustic emission during creep, and (2) a study of the effect of residual stress level on the magnitude of the acoustic emission.

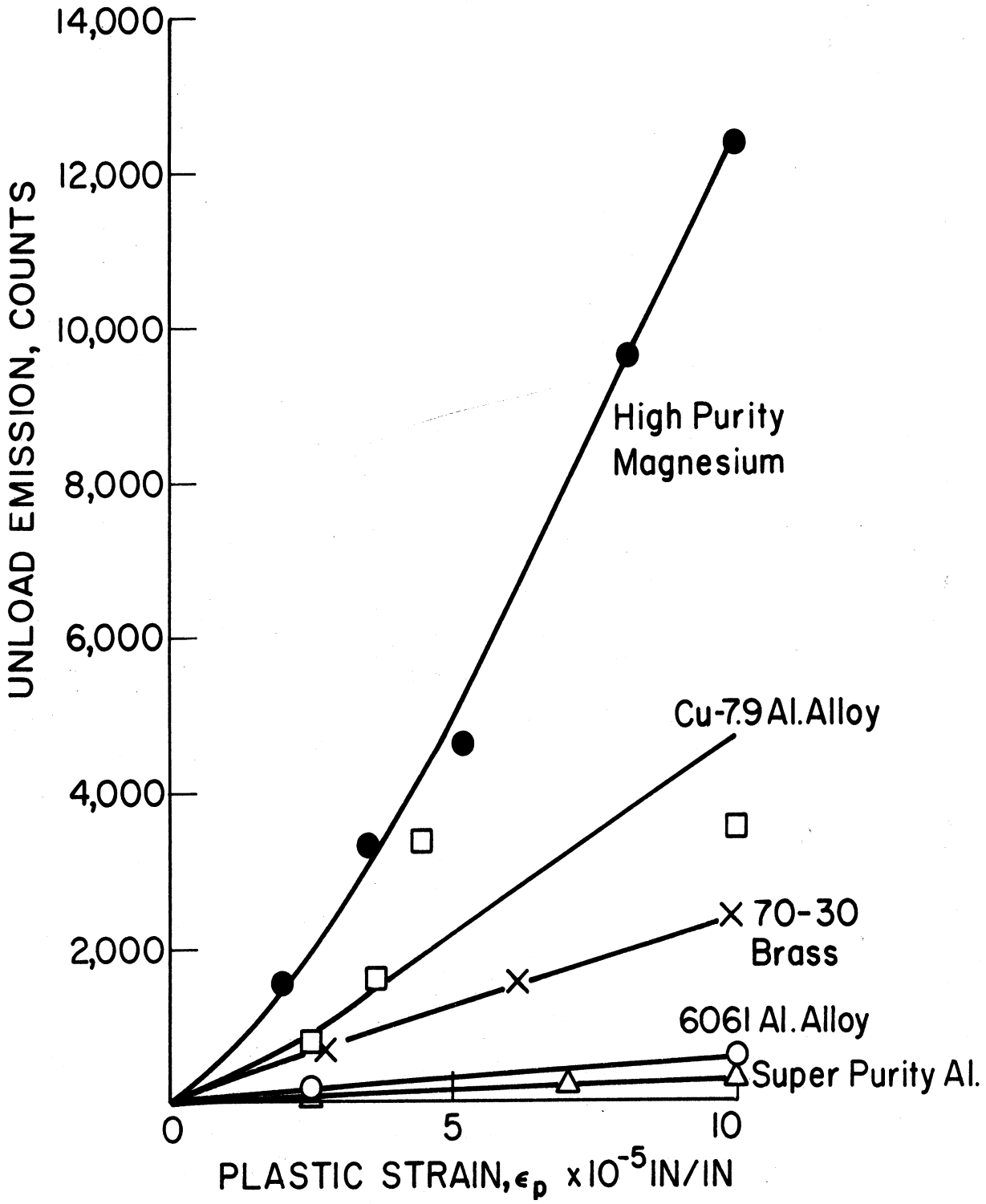


Fig. 4. The unload emission increases as the amount of plastic strain increases. One specimen was used for each curve. An increasing load pattern was used.

## REFERENCES


1. Agarwal, A. B. L., "An Investigation of the Behavior of The Acoustic Emission from Metals and a Proposed Mechanism for Its Generation", Ph.D. dissertation, The University of Michigan, Ann Arbor, Michigan, 1968.

2. Mott, N. F., "A Theory of Work Hardening of Metal Crystals," The Philosophical Magazine, Vol 43, October, 1952.

3. Greetham, G., Honeycombe, R.W.D., "The Deformation of Single Crystals of Aluminum - 4.5 Percent Copper Alloy", J. Inst. Metals, 89, p. 13, 1960-61.

DISTRIBUTION LIST

(One copy unless otherwise noted)

AFML/MAMN 3
Attn: Lt. James W. Bohlen
Wright-Patterson Air Force Base
Ohio 45433

Defense Documentation Center 20
Cameron Station
Alexandria, Virginia 22314

Director 3
Advanced Research Projects Agency
Washington, D.C. 20301

Dr. George Martin
North American Rockwell Corporation
Los Angeles Division
International Airport
Los Angeles, California 90009

Mr. Phil Crimmins
Aerojet-General Corporation
Sacramento, California 95813

Dr. J. R. Frederick
The University of Michigan
Department of Mechanical Engineering
2046 East Engineering Building
Ann Arbor, Michigan 48105

Professor R. H. Chambers
Department of Physics
Engineering Experiment Station
University of Arizona
Tuscon, Arizona 85721

Mr. Darrell James
Department of Metallurgy
College of Engineering
University of Denver
University Park
Denver, Colorado 80210

Mr. Eugene Roffman
Frankford Arsenal
Fire Control Laboratories
Philadelphia, Pennsylvania 19137

Mr. Solomon Goldspiel
U. S. Naval Applied Science
Laboratory
Flushing and Washington Avenues
Brooklyn, New York 11251

Mr. Otto Gericke
Test and Evaluation Methods
Army Material Command
Army Materials and Mechanics Research
Center
Watertown, Massachusetts 02172

Lt. Col. Louis Klinker, U. S. Army
Office Chief of Research and De-
velopment
Materials Science and Technology
Branch
Highland Building
3045 Columbia Pike
Arlington, Virginia 22204

Mr. Edward Criscuolo
Naval Ordnance Laboratory
Radiation Physics Division
Attn: Code 223
White Oak
Silver Spring, Maryland 20910

Mr. Stephen D. Hart
Naval Research Laboratory
Mechanics Division
Washington, D.C. 20390

Mr. F. S. Williams
Aero Materials Department
Naval Air Development Center
Warminston, Pennsylvania 18974

Dr. A. S. Tetelman, Head
Materials Division
College of Engineering
University of California
Los Angeles, California 90024

Dr. L. W. Orr
Department of Electrical Engineering
The University of Michigan
Ann Arbor, Michigan 48105

Professor Emmett N. Leith
Department of Electrical Engineering
The University of Michigan
Ann Arbor, Michigan 48105

J. L. Kreuzer
Optical Group
Perkin-Elmer
Norwalk, Connecticut 06850

D. D. Skinner
Fellow Engineer
Westinghouse Electric Corporation
Research Laboratories
Pittsburgh, Pennsylvania 15235

Dr. Volker Weiss
Associate Chairman
Department of Chemical Engineering
and Metallurgy
Syracuse University
Syracuse, New York 13210

Robert C. McMasters
Nondestructive Testing Research
Laboratory
Department of Welding Engineering
Ohio State University
Columbus, Ohio 43210

Professor Lawrence Mann, Jr.
Department of Mechanical, Aerospace,
and Industrial Engineering
Louisiana State University
Baton Rouge, Louisiana 70803

Howard A. Johnson
The Boeing Company
Space Division, Aerospace Group
Kent Facility
P. O. Box 3868
Seattle, Washington, 98124

W. Lyle Donaldson
Southwest Research Institute
8500 Colebra Road
San Antonio, Texas 78206

Mr. Carlton H. Hastings
Chief, NDT Evaluation
AVCO Corporation
Space Systems Division
Lowell Industrial Park
Lowell, Massachusetts 01851

Mr. David Driscoll
U. S. Army Materials and Mechanics
Research Center
Watertown, Massachusetts 02172

Dr. R. L. Gause
Materials Division
Marshall Space Flight Center
Huntsville, Alabama 35800

The Institute for Defense Analysis
400 Army-Navy Drive
Arlington, Virginia 22202

The Nondestructive Testing
Information Service
Watertown Arsenal
Watertown, Massachusetts 02172

Pravin G. Bhuta, Manager
Applied Mechanical Laboratory
Systems Group of TRW, Inc.
1 Space Park
Redondo Beach, California 90278

Allen Green
Aerojet-General Corporation
Materials Integrity Group
Dept. 0729, Bldg. 2931
Sacramento, California 95813

T. Theodore Anderson
Argonne National Laboratory
Reactor Engineering Division, D308
9700 S. Cass Avenue
Argonne, Illinois 60439

Phil Hutton
Battelle-Northwest
P. O. Box 999
Richland, Washington 99352

Robert Moss
Boeing Scientific Research Laboratory
1-8000, MS 01-14
P. O. Box 3981
Seattle, Washington 98124

Charles Musser
The Boeing Company
Saturn Booster Branch
Org. 5-1752, MS LE-62
P. O. Box 29100
New Orleans, Louisiana 70129

Harvey L. Balderston
The Boeing Company
Space Division, Kent Facility
Org. 2-5022, MS 84-38
P. O. Box 3868
Seattle, Washington 98124

Thomas F. Drouillard
Dow Chemical Company
Rocky Flats Division
P. O. Box 888
Golden, Colorado 80401

Dwight Parry
Phillips Petroleum
P. O. Box 2067
Idaho Falls, Idaho 83401

R. E. Ringsmith
Jet Propulsion Laboratory
California Institute of Technology
4800 Oak Grove Drive
Pasadena, California 91103

Brad Schofield
Teledyne Materials Research
303 Bear Hill Road
Waltham, Massachusetts 02154

Hal Dunegan
University of California
Lawrence Radiation Laboratory
P. O. Box 808
Livermore, California 94550

C. D. Bailey
Lockheed-Georgia Company
Materials Development Laboratory
Department 72-14
Marietta, Georgia 30060

R. F. Saxe
North Carolina State University
Nuclear Engineering Department
P. O. Box 5636
Raleigh, North Carolina 27607

A. W. Porter
Government of Canada
Forest Products Laboratory
6620 N.W. Marine Drive
Vancouver 8, British Columbia, Canada

A. A. Pollock
Linctec, Ltd.
Staple House, 51-52 Chancery Lane
London, WC 2, England